Effects of zinc carnosine on bone loss in mice with diabetic osteoporosis

JINGYUAN GAO[1*], HAO YANG[1,2*], QIANGQIANG LIAN[2], YUNPENG HU[2], ZHOU YANG[2], LEI XING[1,2], YING XUE[2], XIAOLI HOU[2], FAMING TIAN[2] and DONG HU[3]

[1]Department of General Practice Medicine, Affiliated Hospital of North China University of Science and Technology, Tangshan, Hebei 063000, P.R. China; [2]School of Public Health, Hebei Key Laboratory for Organ Fibrosis Research, North China University of Science and Technology, Tangshan, Hebei 063210, P.R. China; [3]Department of General Practice Medicine, Xiangshan Red Cross Taiwan Compatriot Hospital Medical and Health Group, Ningbo, Zhejiang 315600, P.R. China

Received March 26, 2025; Accepted August 20, 2025

DOI: 10.3892/mmr.2025.13723

Abstract. Diabetic osteoporosis (DOP) is on the rise globally, presenting a notable healthcare challenge due to its complex pathogenesis and high fracture risk. Currently, available treatments have limitations, highlighting an urgent need for novel therapeutic approaches. Zinc carnosine (ZnC), a compound formed by the chelation of carnosine with trace-element zinc ions, has shown potential in inhibiting the accumulation of advanced glycation end products in the bone microenvironment, yet its effects on DOP remain under-explored. The present study aimed to examine the effects of ZnC on bone loss in a mouse model of DOP. A total of 24 male mice, aged 6 weeks, were assigned to control, type 2 diabetes mellitus (T2DM) and ZnC intervention groups. DOP was induced using a high-fat diet combined with streptozotocin (STZ). Following 8 weeks of treatment with ZnC at a dosage of 100 mg/kg/day, bone parameters were evaluated using micro-computed tomography (micro-CT), histological staining and molecular analyses. The micro-CT analysis revealed that bone mineral density (BMD), bone volume/tissue volume (BV/TV), number of bone trabeculae (Tb.N), thickness of cortical bone (Ct.Th) and area of cortical bone (Ct.Ar) were significantly lower in the T2DM model group compared with that in the control group ($P<0.05$). Conversely, bone trabecular separation (Tb.Sp) structural model index (SMI) and porosity of cortical bone (Ct.Po) were significantly higher in the T2DM model group compared with those in the control group ($P<0.05$). The ZnC intervention group showed significant increases in BMD, BV/TV, Tb.N, Ct.Th and Ct.Ar, and significant decreases in Tb.Sp compared with the T2DM model group. Tartrate-resistant acid phosphatase staining demonstrated a notable reduction in osteoclast numbers in the ZnC intervention group relative to the T2DM model group. Furthermore, immunohistochemical staining and reverse transcription-quantitative PCR indicated an upregulation of osteoblastic markers, including type I collagen, osteocalcin and osteoprotegerin, alongside a downregulation of the osteoclastic marker receptor activator of nuclear factor-κB ligand in the ZnC group. In conclusion, ZnC supplementation was shown to mitigate bone loss in DOP by promoting bone formation and reducing bone resorption. This was evidenced by enhancements in bone microstructure, a reduction in osteoclast activity and favorable changes in bone metabolism markers. These findings underscore the potential of ZnC as a therapeutic option for bone diseases associated with diabetes.

Correspondence to: Mr. Dong Hu, Department of General Practice Medicine, Xiangshan Red Cross Taiwan Compatriot Hospital Medical and Health Group, 420 Shipufengxi Road, Ningbo, Zhejiang 315600, P.R. China
E-mail: hunguilingyu@qq.com

Professor Faming Tian, School of Public Health, Hebei Key Laboratory for Organ Fibrosis Research, North China University of Science and Technology, 21 Bohai Road, Caofeidian, Tangshan, Hebei 063210, P.R. China
E-mail: tfm9911316@163.com

*Contributed equally

Abbreviations: ZnC, zinc carnosine; DOP, diabetic osteoporosis; T2DM, type 2 diabetes mellitus; STZ, streptozotocin; micro-CT, micro-computed tomography; BMD, bone mineral density; BV/TV, bone volume/tissue volume; Tb.N, number of bone trabeculae; Ct.Th, thickness of cortical bone; Ct.Ar, area of cortical bone; Tb.Sp, bone trabecular separation; Ct.Po, porosity of cortical bone; ROS, reactive oxygen species; ROI, region of interest; Tb.Th, bone trabecular thickness; SMI, structural model index; Max-Load, maximum load; COL-I, type I collagen; OCN, osteocalcin; AOD, average optical density value; FBG, fasting blood glucose

Key words: zinc carnosine, diabetic osteoporosis, bone mineral density, bone microstructure parameters, streptozotocin

Introduction

Diabetes mellitus has emerged as a major global health concern, with its prevalence steadily rising. According to the International Diabetes Federation, the global prevalence of diabetes was estimated at 10.5% (536.6 million people) in 2024, and projections indicate that it will increase to 12.2%

(783.2 million people) by 2045 (1). Diabetic osteoporosis (DOP), a notable complication of diabetes, is becoming increasingly prevalent (2). Epidemiological data reveals the gravity of the situation. A meta-analysis of 21 studies involving 11,603 patients with type 2 diabetes mellitus (T2DM) found a high osteoporosis prevalence of 27.67% (95% confidence interval, 21.37-33.98%) (3). Another study reported that >35% of patients with diabetes experience bone loss, with ~20% meeting the diagnostic criteria for osteoporosis (4). The incidence of fractures, a severe consequence of DOP, is also notably high. In patients with type 1 diabetes mellitus, the relative risk for hip fracture was reported as 4.93 (95% confidence interval, 3.06-7.95), while in patients with T2DM the risk was 1.33 (95% confidence interval, 1.19-1.49) (5).

The pathogenesis of DOP is primarily attributed to either absolute or relative insulin deficiency, which leads to the formation and accumulation of advanced glycation end products (AGEs) (6,7). These AGEs disrupt the cross-linking of collagen in the bone matrix, resulting in alterations to bone microstructure, decreasing bone density per unit volume, decreasing bone strength and increasing bone fragility, thereby compromising bone quality in diabetic patients and elevating the risk of fractures (8,9). In current medical practice, the traditional medical treatment of DOP has certain limitations (10). For instance, drugs such as thiazolidinediones may affect bone metabolism and increase the risk of fractures. Although insulin has the effect of promoting bone synthesis, observational studies have shown that the fracture risk also increases in insulin users (11). The therapeutic effects of some drugs are not satisfactory, and the efficacy of these drugs in treating related complications and the applicable population remain unclear. Further research is needed to clarify these aspects (12). Over the years, numerous animal models have been established to study the pathophysiology of T2DM-associated osteoporosis. For instance, the combination of a high-fat diet and streptozotocin (STZ) in rodents has been widely used to induce T2DM-like conditions, which are then associated with subsequent development of osteoporosis-like bone changes (13,14). These models have shown characteristic features such as reduced bone mineral density (BMD), deteriorated bone microstructure and imbalanced bone remodeling, closely mimicking the human DOP phenotype (15,16).

Zinc carnosine (ZnC), also known as polaprezinc, is an orally available biochelate composed of L-carnosine and zinc ions (17). ZnC is broken down during intestinal absorption into two compounds: L-carnosine and zinc. Carnosine, a naturally active dipeptide, is abundant in mammalian skeletal muscle and brain, and is synthesized in the body from β-alanine and L-histidine. Zinc exhibits a range of beneficial properties, including anti-inflammatory, antioxidant, anti-aging, antitumor and immune regulatory effects, the scavenging of oxygen free radicals, prevention of AGEs, chelation of bivalent metal ions (such as $zinc^{2+}$ and $copper^{2+}$), and anti-protein carboxylation and anti-glycosylation effects (18-20). Studies have confirmed that carnosine can effectively reduce reactive oxygen species (ROS) levels in chondrocytes injured by hydrogen peroxide (H_2O_2), thereby inhibiting chondrocyte degeneration and bone loss (21,22). Zinc is an important trace element necessary for the growth, development and maintenance of bone health, and it is considered a key factor in bone metabolism (23). Additionally, zinc ions exhibit anti-glycosylation and anti-oxidation effects (24,25). Research has shown that zinc ions can promote the differentiation of human bone marrow mesenchymal stem cells and mouse bone marrow monocytes into osteoblasts and osteoclasts (26). By mediating the receptor activator of nuclear factor-κB ligand (RANKL)/RANK/osteoprotegerin (OPG) and Wnt signaling pathways, zinc ions positively influence bone metabolism by upregulating the expression of key genes involved in bone formation (20,27,28). In the latest review by Yudhani *et al* (29), zinc was summarized to play a notable role in alleviating obesity, particularly in lipid metabolism, appetite regulation, insulin signaling and inflammatory responses.

The present study aims to fill this research gap by focusing on ZnC. The originality of the present study lies in comprehensively evaluating the potential of ZnC in ameliorating DOP. To the best of our knowledge, previous studies have not examined the effects of ZnC in its chelated form on DOP, and did not conduct a thorough investigation into the complex pathophysiological processes of DOP. The present study explores the effects of ZnC on bone loss and bone quality in a T2DM mouse model through a multi-parameter assessment, including imaging, biomechanics, histology and molecular biology analysis. By doing so, the present study aims to provide novel insights into the treatment of DOP and potentially identify ZnC as a new therapeutic option.

In conclusion, AGEs induced by T2DM trigger oxidative stress, stimulate the production of inflammatory cytokines and ROS, and provoke an inflammatory response in osteoblasts and osteoclasts. This cascade of events induced by AGEs enhances the bone resorption activity of osteoclasts, thereby contributing to the development of DOP (30,31). Both L-carnosine and zinc ions exhibit notable antioxidation and anti-glycosylation effects and are closely associated with bone metabolism. The chelation of carnosine with trace element zinc ions forms ZnC, which may inhibit the accumulation of AGEs in the bone microenvironment by clearing ROS. The removal of ROS could reduce the persistent progression of chronic low-level inflammation in a high-glucose environment, lower the expression of inflammatory factors that induce insulin resistance and decrease osteoblast apoptosis, thereby ameliorating osteoporosis both directly and indirectly (32,33). The present study employed a T2DM mouse model to investigate the impact and mechanism of oral ZnC supplementation on DOP. The present investigation was based on evidence of bone loss and deteriorating bone quality in diabetic mice and assessed various parameters, including imaging, biomechanics, histology and molecular biology analysis results.

Materials and methods

Experimental animals. All experimental protocols were conducted in compliance with the requirements of the Animal Ethics Committee and have been approved by the Experimental Animal Ethics Committee of North China University of Science and Technology (Tangshan, China; approval no. 2023-SY-230). A total of 24 specific pathogen-free (SPF) C57BL/6J 6-week-old male mice were purchased from Beijing Huafukang Biotechnology Co., Ltd. The mice were housed under standard conditions at a temperature of 22±2˚C

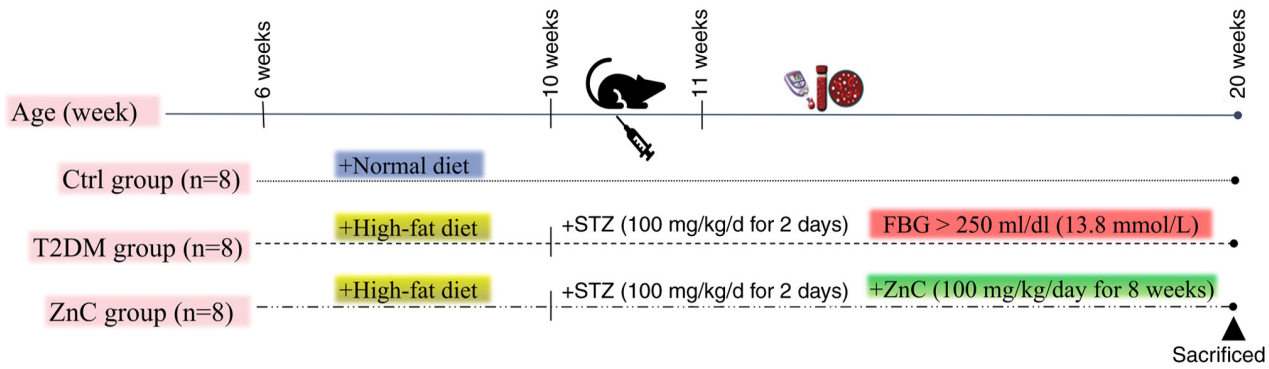

Figure 1. Schematic diagram of experimental modeling. Ctrl, control; T2DM, type 2 diabetes mellitus; ZnC, zinc carnosine; STZ, streptozotocin; FBG, fasting blood glucose; w, week; d, day.

and a humidity of 50±5%, with a 12-h light/12-h dark cycle, ensuring access to adequate water. The mean body weight of the mice was ~18±3 g and they were fed with a standard diet for 1 week to allow for adaptation.

Animal modeling and grouping. A total of 24 6-week-old SPF male C57BL/6J mice were used in the experiment. The mice were randomly divided into 3 groups, with 8 mice in each group. During the experiment, general observations were conducted on the animals every day, including appearance, behavior and activity status. A detailed examination was performed once a week, including measuring body weight, observing eating and drinking habits, and checking for any disease symptoms. If abnormal behaviors were observed in the animals, such as lethargy, reduced activity or diarrhea, the observation frequency was increased. In the present experiment, anesthetic agents were not administered during the observation and handling procedures, as these did not involve invasive interventions. All mice survived until the end of the experiment and no mice died.

The experiment lasted for 20 weeks, starting from week 1 and ending at week 20. In the first 4 weeks, 16 mice were fed a high-sugar and high-fat diet to induce metabolic disorders of sugar, fat and insulin resistance. Subsequently, starting from week 5, 12 h of fasting was followed by intraperitoneal injections of STZ at a dose of 100 mg/(kg/day) for 2 consecutive days. STZ was dissolved in 0.1 mol/l citrate-sodium citrate buffer (pH 4.5). This treatment was designed to damage pancreatic β cells and establish a model of T2DM. The control group received standard food and was intraperitoneally injected with citrate-sodium citrate buffer (0.1 mol/l; pH 4.5) as a pH-matched control vehicle at week 5 (34-36). This ensured that any observed differences could be attributed to the effects of STZ or ZnC (33,37,38). After completion of the STZ injections, the fasting blood glucose (FBG) levels of the mice were monitored on designated days. Mice with FBG levels >250 mg/dl (13.8 mmol/l) on 3 consecutive days were confirmed as T2DM models. After the successful construction of the model, the ZnC group and the T2DM group underwent corresponding treatments for 8 weeks. The ZnC group was orally administered 100 mg/(kg/day) ZnC, while the T2DM group was orally administered 1 ml/(kg/day) 0.9% sodium chloride solution once daily. At the end of week 20 in the experiment, all mice were euthanized via cervical dislocation. After performing the cervical dislocation, signs such as cessation of breathing, disappearance of heartbeat and dilation of pupils were observed to confirm the death of the animals. At the same time, all experimental mice underwent autopsy to further confirm the death status, ensuring the accuracy of the experimental data and the reliability of the experimental results, and for the collection of tissue samples for subsequent experiments (Fig. 1).

Micro-computed tomography (micro-CT) analysis. The right tibia of each mouse was scanned using high-resolution micro-CT (SkyScan1176; Bruker Corporation) to assess BMD and microstructural parameters. The scanned images were reconstructed and analyzed using Avatar software [version 1.7.4.0; Pingseng Medical Technology (Kunshan) Co., Ltd.]. For trabecular bone, the region of interest (ROI) was defined as starting at 0.2 mm distal to the growth plate and extending 5% of the tibial length distally, thereby excluding the growth plate and primary spongy body. The following parameters were obtained: BMD (g/cm^3) bone volume/tissue volume (BV/TV; %), number of bone trabeculae (Tb.N; 1/mm), bone trabecular thickness (Tb.Th; μm), bone trabecular separation (Tb.Sp; mm) and structural model index (SMI). For cortical bone, the ROI for selected scans commenced at 40% of the tibia length distal to the proximal growth plate and extended 10% of the tibia length distally. Within this ROI, thickness of cortical bone (Ct.Th; μm), area of cortical bone (Ct.Ar, %) and cortical porosity (Ct.Po, %) were calculated. Ct.Ar refers to the absolute cortical bone area within the ROI, while total bone area was not measured in this study.

Determination of biomechanical properties. The right femurs were utilized for biomechanical testing using a universal electronic testing machine (cat. no. MMT-250NV-10; Shimadzu Corporation). The load-measuring accuracy of the testing instrument was 0.01 N, with a span length of 6 mm and a loading speed of 2 mm/min. Based on the load-displacement curve, the maximum load (Max-Load; N) and the maximum bending stress (Max-Stress; N/mm^2) were obtained.

Hematoxylin and eosin (H&E) staining and tartrate-resistant acid phosphatase (TRAP) staining. Left tibial tissues were processed for histological examination using H&E staining and TRAP staining. For bone tissue decalcification, the left

tibia was initially fixed in 4% paraformaldehyde at room temperature (25˚C) for 24 h, followed by decalcification in a 17% EDTA solution at room temperature (25˚C) 12 weeks, with the solution being changed weekly. Section preparation involved a series of steps: Dehydration, clearing, paraffin embedding and embedding utilizing an automatic embedding machine. Paraffin blocks were sectioned at a thickness of 5 μm using a rotary microtome (Leica RM2235, Leica Biosystems). The trimmed wax blocks were subjected to continuous sectioning. First, the sections were pre-cooled on an ice stage to prevent tissue fragmentation, followed by fine trimming. Subsequently, the sections were spread in warm water at 45˚C to obtain flat and wrinkle-free sections. Next, the sections were picked up and placed in a 60˚C oven for overnight drying to ensure tight adhesion. Finally, the dried sections were stored at room temperature for subsequent staining and immunohistochemical experiments.

The tissue sections were placed in an oven at 60˚C and baked for 2 h to remove the wax. Successive immersions were performed in 100% xylene I, 100% xylene II, and 100, 95, 80, 70 and 60% ethanol, with each solution applied for 10 min, to complete the dewaxing and rehydration process. Staining and immunohistochemical experiments were then performed.

H&E staining was performed, which included hematoxylin (cat. no. BL702B; Biosharp Life Sciences) staining at room temperature for 3-5 min, differentiation using a 1% hydrochloric acid solution in ethanol for 20 sec, bluing with 1% ammonia for 5 min, eosin staining (cat. no. BA4098; Zhuhai Beisuo Biotechnology Co., Ltd.) for 30 sec and sealing with neutral gum following dehydration and clearing.

For TRAP staining, a staining solution composed of 0.1 M acetic acid buffer, 1 mg/ml hexazo para-fuchsin and naphthol AS-BI phosphate (all from Sigma-Aldrich, USA) was prepared. Sections were dewaxed, hydrated, stained and incubated for 3 h, after which they were washed, counterstained, differentiated, dehydrated, cleared and sealed to ensure optimal staining quality for subsequent observation and analysis. Histological sections were examined using a BX53 optical microscope (Olympus Corporation) at x40 and x100 magnification. The osteoclast number was obtained by counting the number of TRAP-positive cells (39).

Immunohistochemical staining. After sections that had been dewaxed to water were washed with phosphate buffered saline [PBS; cat. no. AC08L033; Life-iLab; Heyuan Liji (Shanghai) Biotechnology Co., Ltd.] for 10 min, antigen repair was performed by incubation with 0.05% trypsin [cat. no. AC15L821; Life-iLab; Heyuan Liji (Shanghai) Biotechnology Co., Ltd.] at 37˚C for 30 min. To block endogenous peroxidase activity, 3% H_2O_2 was incubated at room temperature for 10 min. The sections were then incubated with the corresponding primary antibody at 4˚C overnight. The primary antibodies used and their dilution ratios are as follows: Type I collagen (COL-I; 1:200; cat. no. AF7001; Affinity Biosciences), osteocalcin (OCN, 1:200; cat. no. 16157-1-AP; Proteintech Group, Inc.) and OPG (1:200; cat. no 31766-1-AP; Proteintech Group, Inc.). The next day, after the sections were rinsed with PBS, they were incubated with secondary antibody (cat. no. 2414D1020; Beijing Zhongshan Jinqiao Biotechnology Co., Ltd.), and diaminobenzidine (cat. no. ZLI-9018; Beijing Zhongshan Jinqiao Biotechnology Co., Ltd.) was used for color development, which was terminated by washing with PBS. After counterstaining with hematoxylin for 1 min, differentiation was performed with 1% hydrochloric acid ethanol for 3 sec, followed by rinsing with tap water for 15 min to return to blue. Subsequently, dehydration was carried out with gradient ethanol at 60, 70, 80, 90 and 100% for 5 min each in sequence, followed by 100% xylene clearing for 5 min and finally mounting with resin. All sections were imaged under an optical microscope (Olympus BX53; Olympus Corporation) at a magnification of x200. The region under the growth plate was selected as the ROI, and Image J software (National Institutes of Health) was used to analyze the average optical density (AOD) within the ROI of each section.

Reverse transcription-quantitative PCR (RT-qPCR). For RT-qPCR, femurs were ground and lysed using Trizol (cat. no. DP424; Tiangen Biotech Co., Ltd.) reagent, at room temperature (25˚C) for 5 min. Chloroform (MilliporeSigma) was added, and the mixture was vortexed for 15 sec and incubated at room temperature for 3 min, followed by centrifugation at 12,000 x g for 15 min at 4˚C to separate the aqueous phase containing RNA. RNA was precipitated by adding isopropyl alcohol, incubated at room temperature for 10 min, and pelleted by centrifugation at 12,000 x g for 10 min at 4˚C. The RNA pellet was washed with 70% ethanol, centrifuged at 7,500 x g for 5 min at 4˚C and air-dried before resuspension in RNase-free water. The purified RNA was dissolved in nuclease-free water, and its concentration and purity were assessed using a UV spectrophotometer (cat. no. SLAN-96S; Shanghai Hongshi Medical Technology Co., Ltd.). A 20-μl reaction mixture was prepared, and first-strand cDNA was synthesized using a reverse transcription kit (cat. no. ZR103; Beijing Zhuangmeng International Biogene Technology Co., Ltd.) according to the manufacturer's protocol. The cDNA was subsequently subjected to qPCR in a 20-μl reaction volume using the SYBR® Premix Ex Taq™ II kit (cat. no. ZR103-1; Beijing Zoman Biotechnology Co., Ltd.) with SYBR Green as the fluorophore. With β-actin as the internal reference gene, the $2^{-\Delta\Delta Cq}$ method (40) was used to calculate the relative mRNA expression levels of the target genes relative to the control group. The genes analyzed included OPG, OCN and RANKL, which were selected since they are key regulators of bone metabolism and remodeling, serving as important markers of osteogenic differentiation and bone turnover. The primer synthesis was completed by Sangon Biotech Co., Ltd. The primer sequences used are shown in Table I. The PCR conditions were as follows: 94˚C for 5 min, followed by 35 cycles of 94˚C for 30 sec, 52-58˚C for 30 sec and 72˚C for 30 sec.

Statistical analysis. All data are presented in the form of mean ± standard deviation. The present study used SPSS 22.0 software (IBM Corp.) for all statistical analyses. For the differences between groups that follow a normal distribution, a one-way analysis of variance (ANOVA) was first used to confirm the overall group differences. If the ANOVA results showed a statistically significant difference ($P<0.05$), then the LSD (least significant difference) post-hoc test was further used to conduct pairwise comparisons between each group to clearly identify which groups had differences. Each group had

Table I. Primer sequences of selected genes.

Gene	Primer sequence (5'-3')
OCN	
Forward	GAGGGCAATAAGGTAGTGAA
Reverse	CATAGATGCGTTTGTAGGC
OPG	
Forward	CAGAGCGAAACACAGTTTG
Reverse	CACACAGGGTGACATCTATTC
RANKL	
Forward	TGTACTTTCGAGCGCAGATG
Reverse	CCACAATGTGTTGCAGTTCC
β-actin	
Forward	GATCAGCAAGCAGGAGTACGA
Reverse	GGTGTAAAACGCAGCTCAGTAAC

OCN, osteocalcin; OPG, osteoprotegerin; RANKL, receptor activator of nuclear factor-κB ligand.

a sample size of 8 mice (n=8), and comparisons were made between groups. The significance level α was set at 0.05. During the analysis, the actual P-value of each test was clearly indicated. P<0.05 was considered to indicate a statistically significant difference; if P≥0.05, it indicated that there was no statistically significant difference between the groups.

Results

Changes in FBG in each group of mice. Notable differences in blood glucose concentrations were observed in the T2DM model group and the ZnC intervention group when compared with the control group. However, there was no notable difference in blood glucose concentration between the ZnC group and the T2DM group, indicating a lack of a substantial hypoglycemic effect following the ZnC intervention (Fig. 2).

Micro-CT analysis of cancellous and cortical bone parameters. The tibial bone tissue of mice was examined using micro-CT, and the three-dimensional reconstruction images revealed the microstructure of both cancellous and cortical bone. The bone microstructure in the control group appeared generally normal. By contrast, the cancellous bone microstructure in the T2DM model group exhibited significant alterations compared with that of the control group, including thinning of the proximal growth plate, a reduction in the number of trabeculae beneath the growth plate, decreased trabecular thickness, increased trabecular spacing, and enhanced separation and thinning of the cortical bone. Quantitative analysis of tibial bone parameters further validated osteoporosis in the T2DM model. Notably, the microstructural changes observed in the tibia of the T2DM model group were significantly mitigated in the ZnC intervention group.

Further analysis of tibial BMD and bone microstructure parameters revealed that compared with the Control group, the BMD, BV/TV, Tb.N, Ct.Th and Ct.Ar in the T2DM model group were significantly decreased (P<0.05). Notably, there

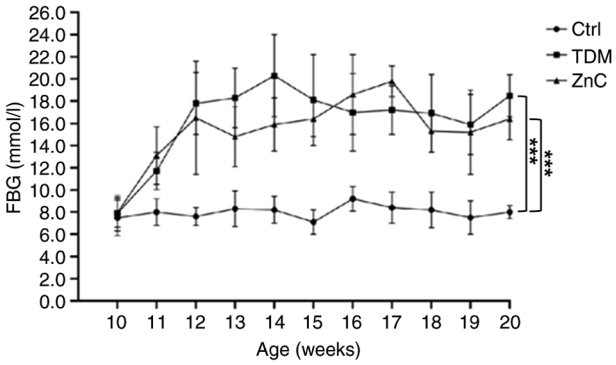

Figure 2. Results of random blood glucose determination in each group of mice. ***P<0.001. Ctrl, control; T2DM, type 2 diabetes mellitus; ZnC, zinc carnosine; FBG, fasting blood glucose.

were no significant differences in SMI, Tb.Th and Ct.Po between the ZnC group and the T2DM model group (P>0.05). However, compared with the T2DM model group, the BMD, BV/TV, Tb.N, Ct.Th and Ct.Ar in the ZnC group were significantly increased, and Tb.Sp was significantly decreased (P<0.05) (Figs. 3 and 4).

Three-point bending test. The biomechanical properties of the femur were assessed using a three-point bending test (Fig. 5). When compared with the control group, the Max-Load in both the T2DM model group and the ZnC intervention group was significantly reduced (P<0.05). However, compared with the T2DM model group, the Max-Load and Max-Stress in the ZnC intervention group were significantly increased (P<0.05).

Histological staining results. Compared with that in the control group, the growth plate in the T2DM model group exhibited a notable reduction in thickness, with considerable damage to the lamellar trabecular structure in the lower bone marrow cavity. The distance between trabeculae increased and the presence of lipid vacuoles was noted. Additionally, the marginal cortical bone was thinner, resulting in a more pronounced loss of total bone mass. By contrast, the ZnC intervention group showed an increase in growth plate thickness, a reduction in the extent of partial destruction of both trabecular and cortical bone and a decrease in total bone mass loss when compared with the T2DM model group (Fig. 6). This is consistent with the results shown in Fig. 4: that is, compared with the control group, BMD, BV/TV, Tb.N, Ct.Th and Ct.Ar in the T2DM model group were all significantly decreased (P<0.05); while ZnC intervention could significantly reverse these indicators (P<0.05).

TRAP staining. Compared with the control group, the T2DM model group exhibited a significantly higher density of TRAP-positive multinucleated cells (≥3 nuclei/cell) (P<0.01) localized predominantly in osteoclast-active regions; specifically, beneath the growth plate and adjacent to the medullary cavity along trabecular surfaces (P<0.05). This pattern indicated enhanced osteoclast-mediated bone resorption in diabetic conditions. Conversely, ZnC intervention significantly suppressed osteoclastogenesis, evidenced by a marked reduction

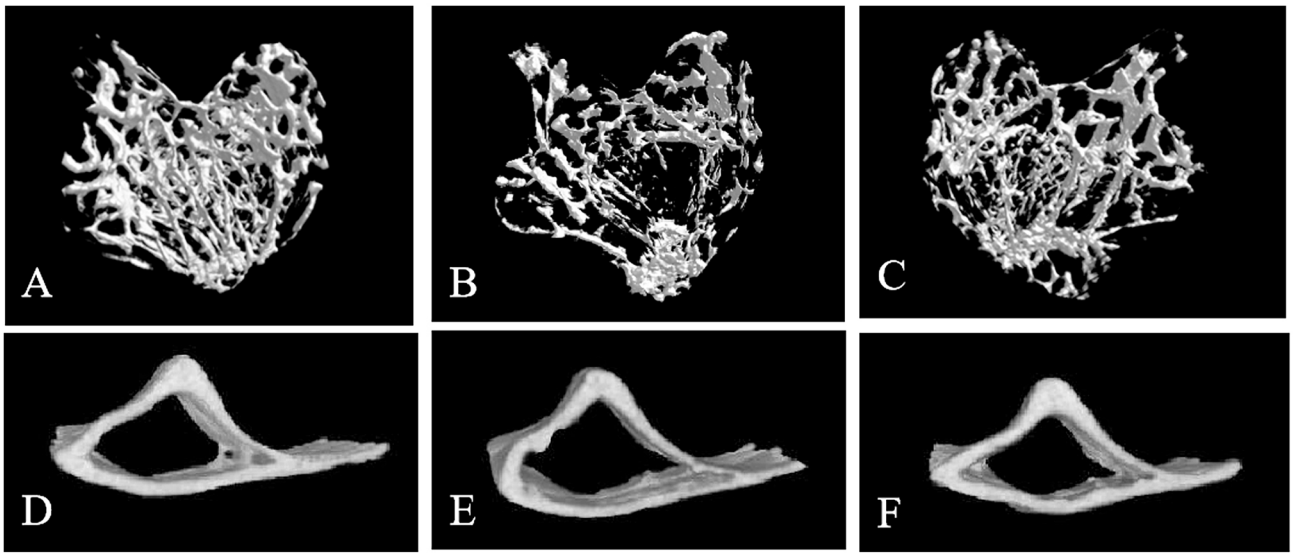

Figure 3. Three-dimensional image reconstruction of mouse tibia by micro-CT. (A-C) Trabecular reconstruction images of each group and (D-F) cortical bone reconstruction images of each group. (A and D) Control group, (B and E) type 2 diabetes mellitus model group (C and F) zinc carnosine intervention group.

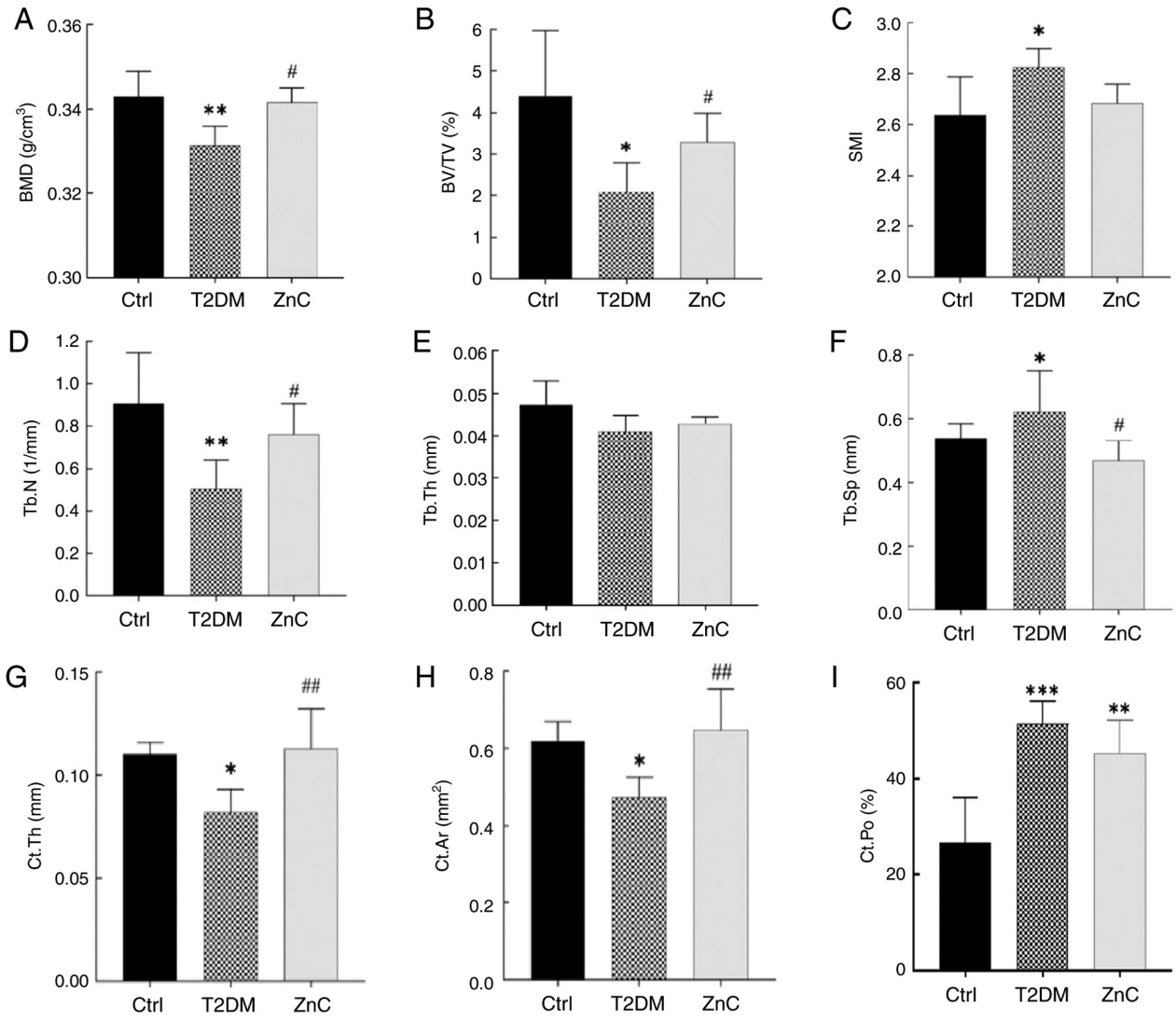

Figure 4. Analysis of tibial BMD and bone microstructure parameters in mice. *P<0.05, **P<0.01 and ***P<0.001 vs. Ctrl group; $^{\#}$P<0.05 and $^{\#\#}$P<0.01 vs. T2DM model group. (A) BMD, bone mineral density; (B) BV/TV, bone volume/tissue volume; (C) SMI, structural model index; (D) Tb.N, number of bone trabeculae; (E) Tb.Th, bone trabecular thickness; (F) Tb.Sp, bone trabecular separation; (G) Ct.Th, thickness of cortical bone; (H) Ct.Ar, area of cortical bone; (I) Ct.Po, porosity of cortical bone. Ctrl, control; T2DM, type 2 diabetes mellitus; ZnC, zinc carnosine.

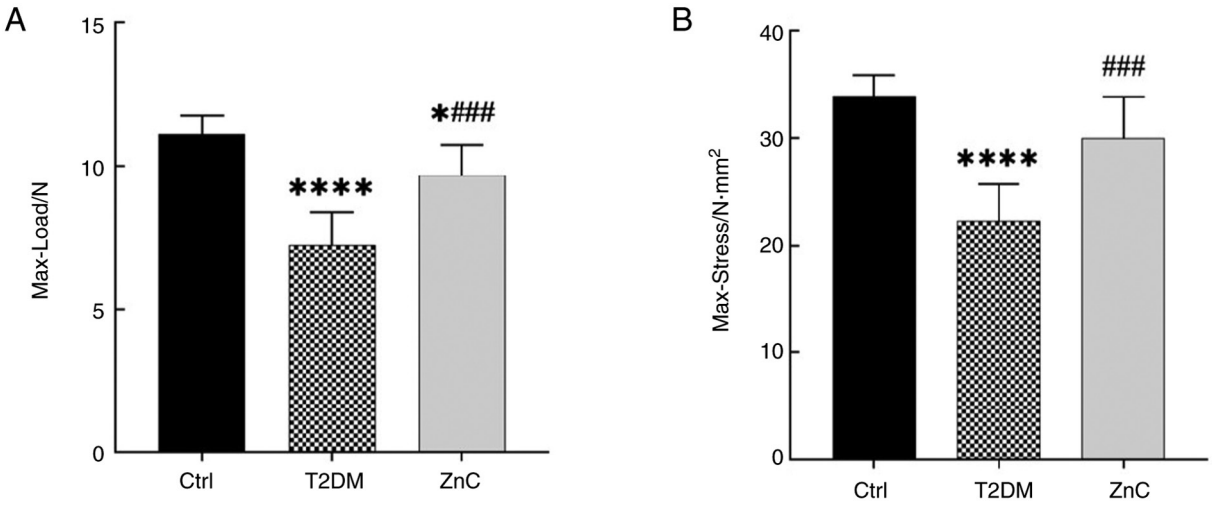

Figure 5. Biomechanical indexes of mice in each group. (A) Max-Load and (B) Max-Stress. *P<0.05 and ****P<0.0001 vs. Ctrl group; $^{###}$P<0.001 vs. T2DM model group. Ctrl, control; T2DM, type 2 diabetes mellitus; ZnC, zinc carnosine; Max-Load, maximum load; Max-Stress, maximum stress.

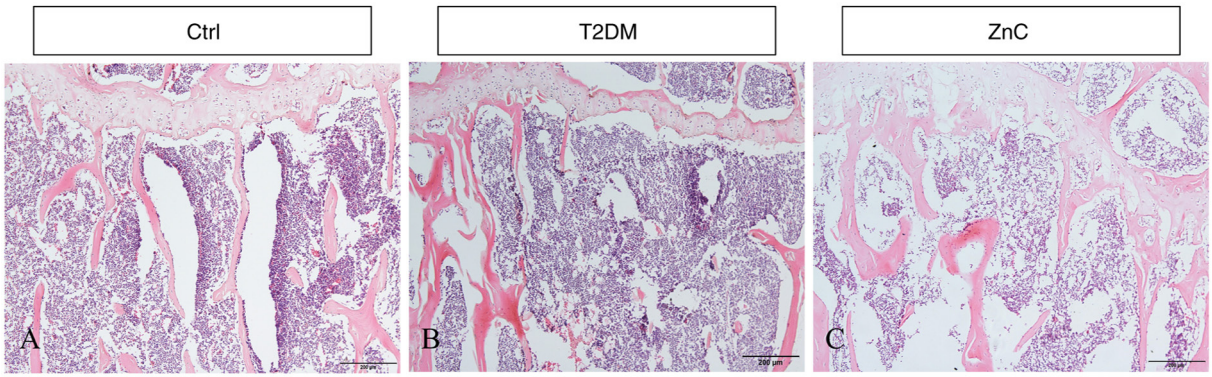

Figure 6. Hematoxylin and eosin staining of tibia in mice of each group (x100 magnification). (A) Control group, (B) type 2 diabetes mellitus model group and (C) zinc carnosine intervention group. Scale bar, 200 μm.

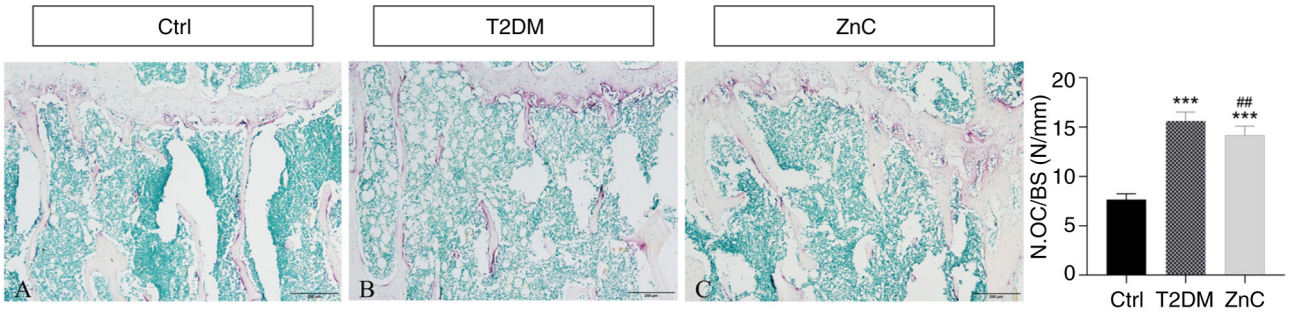

Figure 7. Tartrate-resistant acid phosphatase staining of tibia of mice in each group after 8 weeks of ZnC intervention (x100 magnification). (A) Ctrl group, (B) T2DM model group and (C) ZnC intervention group. The osteoclasts were obtained by counting the number of TRAP-positive cells (N. Trap+). Scale bar, 200 μm. ***P<0.001 vs. Ctrl group; $^{##}$P<0.01 vs. T2DM model group. Ctrl, control; T2DM, type 2 diabetes mellitus; ZnC, zinc carnosine; N.OC, osteoclast number; BS, bone surface.

in TRAP-positive cell density relative to the T2DM model group (P<0.05), as quantified by histomorphometric parameter of measuring osteoclast number/bone surface (41,42) (Fig. 7).

Immunohistochemical detection of protein expression of bone metabolism-related factors in each group. Protein expression of bone metabolism-related factors was evaluated in each group via immunohistochemistry. Quantitative analysis of histochemical staining images revealed no significant differences in the expression levels of bone formation markers type I collagen (COL-I), osteocalcin (OCN) and OPG between the T2DM group and the control group (all P>0.05). By contrast, the AOD of RANKL, a key osteoclast-activating factor, was significantly elevated in the T2DM group compared with that in the control group (P<0.05).

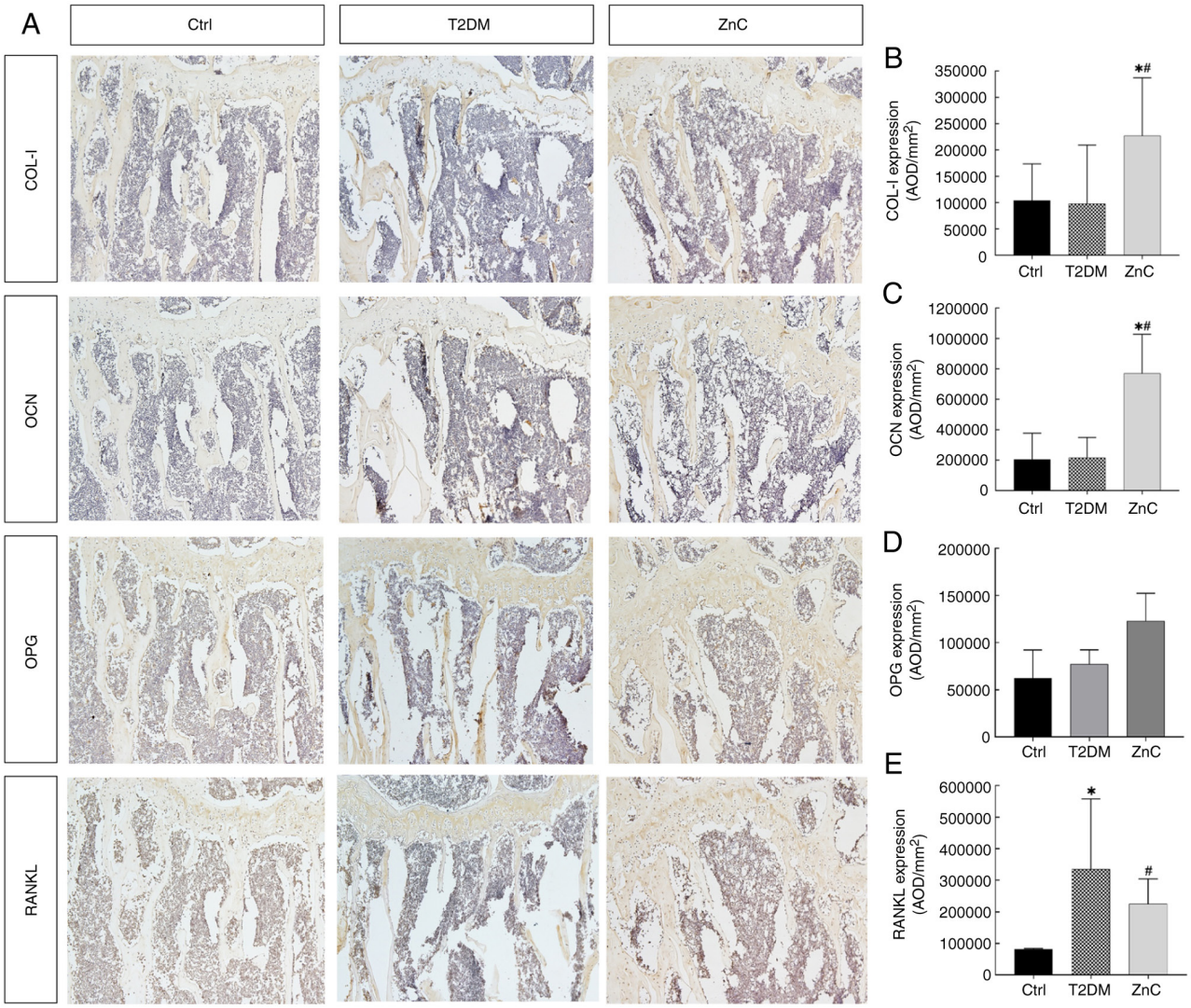

Figure 8. COL-I, OCN, OPG and RANKL protein expression levels in each group after 8 weeks of intervention. (A) COL-I, OCN, OPG and RANKL protein expression level of each treatment group. Average optical density of (B) COL-I, (C) OCN, (D) OPG and (E) RANKL in each group. *P<0.05 vs. Ctrl group; #P<0.05 vs. T2DM model group. COL-I, type I collagen; OCN, osteocalcin; OPG, osteoprotegerin; RANKL, receptor activator of nuclear factor-κB ligand; Ctrl, control; T2DM, type 2 diabetes mellitus; ZnC, zinc carnosine; AOD, average optical density value.

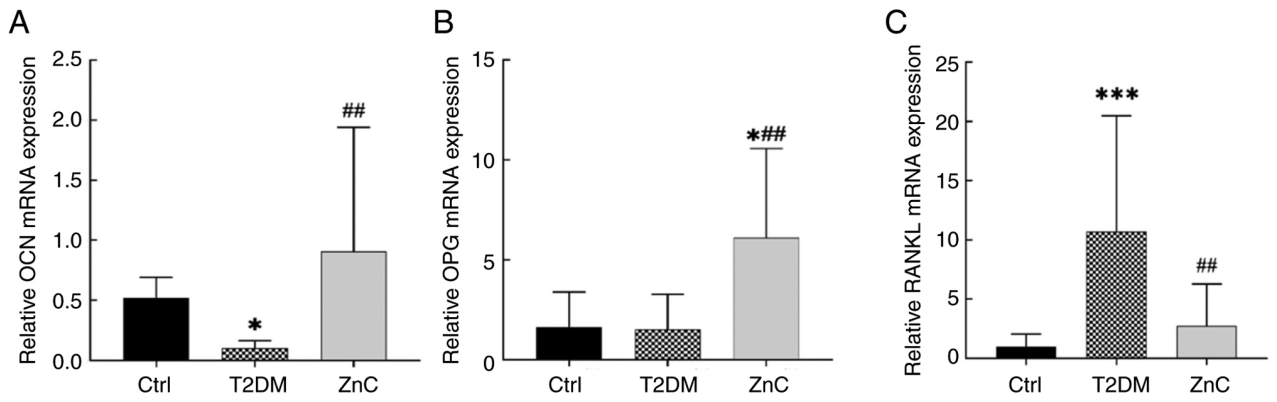

Figure 9. mRNA expression levels of bone metabolism-related factors. *P<0.05 and ***P<0.01 vs. Ctrl group; ##P<0.01 vs. T2DM model group. (A) Ctrl, control; (B) T2DM, type 2 diabetes mellitus; (C) ZnC, zinc carnosine. OCN, osteocalcin; OPG, osteoprotegerin; RANKL, receptor activator of nuclear factor-κB ligand.

Following ZnC intervention, the AOD of osteogenic genes COL-I and OCN increased significantly compared with that in both the control and T2DM groups (all P<0.05), indicating enhanced bone formation. Meanwhile, OPG expression remained unchanged (P>0.05). Notably, ZnC treatment significantly suppressed RANKL expression compared with

that in the T2DM model group ($P<0.05$), suggesting inhibition of osteoclast-mediated bone resorption (Fig. 8).

mRNA expression levels of bone metabolism-related factors. Compared with the control group, the mRNA expression of OCN in mice of the T2DM model group was significantly decreased ($P<0.05$), while the difference in the expression level of OPG was not statistically significant ($P>0.05$); however, the expression level of RANKL was significantly increased ($P<0.05$). When compared with the T2DM group, the ZnC group exhibited significant upregulation of OCN and OPG mRNA expression ($P<0.05$), and downregulation of RANKL mRNA expression ($P<0.05$) (Fig. 9).

Discussion

ZnC is a zinc peptide that is widely used in the treatment of peptic ulcers, gastrointestinal tumors, Alzheimer's disease, diabetes complications and other diseases, and its safety and lack of toxicity have been demonstrated (43,44).

In the present study, a mouse model of DOP was established by administering a high-fat diet in conjunction with intraperitoneal injections of a moderate dose of STZ (45,46). Continuous monitoring of FBG levels and body mass changes confirmed the onset of insulin resistance after 4 weeks of high-fat diet feeding. Following two consecutive injections of moderate doses of 100 mg/(kg/day) STZ, blood glucose levels gradually increased over the course of 1 week, successfully establishing the T2DM model. In the present study, it was observed that the FBG levels of mice receiving ZnC intervention for 8 weeks were lower than those of the diabetes model group without ZnC intervention; however, this difference was not statistically significant, suggesting that ZnC does not have a notable hypoglycemic effect. Previous meta-analyses have indicated that ZnC may possess therapeutic potential in diabetes, as it can reduce glycated hemoglobin and FBG levels (47,48). Further studies are necessary to conclusively determine whether ZnC has a hypoglycemic effect.

ZnC has been demonstrated to markedly alleviate bone mass loss associated with postmenopausal osteoporosis, senile osteoporosis, apraxia osteoporosis, autoimmune osteoporosis and secondary osteoporosis resulting from vitamin D or calcium deficiency (49-52). In the present study, micro-CT analysis revealed that BMD, BV/TV, Tb.N, Ct.Th and Ct.Ar were significantly reduced in the diabetes model group, whilst Tb.Sp, SMI and the Ct.Po were significantly increased compared with the control group. After ZnC intervention, these parameters were partially restored toward control group levels, showing significant improvement compared with the T2DM group. The data of the three-point bending mechanics test indicated that the Max-Load and Max-Stress of the diabetic model group were significantly reduced compared with those of the control group. No significant differences were observed between the ZnC intervention group and the T2DM model group, indicating that ZnC treatment did not significantly improve femoral biomechanical properties. The aforementioned results showed that STZ injection combined with a high-fat diet for 8 weeks could induce a significant DOP phenotype in mice and that the associated osteoporosis was significantly improved after ZnC intervention. ZnC intervention partially mitigated diabetic bone mass loss, as evidenced by improvements in bone microstructure and histological parameters, although biomechanical properties were not significantly restored.

ZnC, a bidirectional modulator, may help to treat osteoporosis and other bone diseases. By increasing the expression levels of protein kinase and protein phosphatase in osteoblasts, ZnC stimulates newly synthesized bone proteins in osteoblasts, enhances the activity of zinc-activated aminoacyl-tRNA synthetase in translation, and stimulates bone formation and calcification (51,53-55). ZnC can also upregulate the OPG/RANKL ratio and block the RANKL/RANK interaction between osteoclast precursors and osteoclasts, thereby effectively inhibiting the formation, differentiation and apoptosis of osteoclasts, and mitigating DOP-associated bone loss (56-60). In the present study, immunohistochemical and histological analyses demonstrated that oral supplementation of 100 mg/(kg/day) ZnC alleviated diabetes-induced bone loss, improved high sugar-induced abnormalities in bone microstructure, and regulated bone metabolism-related factors by increasing osteogenic proteins (COL-I, OCN and OPG) and decreasing the osteoclast-related factor RANKL, accompanied by a reduction in TRAP-positive cells, which may reduce the stimulating effect of diabetes on osteoclast differentiation by promoting osteoblast differentiation, and inhibiting osteoclast differentiation and bone resorption function, and exhibits a protective role in cortical bone and cancellous bone during abnormal bone loss.

In conclusion, ZnC effectively alleviated the DOP phenotype in diabetic mice, improved bone homeostasis and mitigated the abnormal osteoclast activity under the high glucose-metabolic state. ZnC was shown to inhibit bone resorption and promote bone formation by suppressing osteoclast activity and enhancing osteoblast differentiation, demonstrating its potential as a therapeutic drug for bone remodeling-related diseases (including osteoporosis). However, the present study also had certain limitations, as follows: i) The present study was conducted only in mouse models, and the animal-based experimental results exhibit a level of uncertainty when extrapolated to humans; and ii) although the present study explored the effects of ZnC on bone metabolism-related factors and initially revealed its mechanism of action, the specific molecular signaling pathways have not been fully clarified. Future research should consider conducting clinical studies to verify the efficacy and safety of ZnC in humans; at the same time, in-depth explorations of its mechanism of action at the cellular and molecular levels can provide a theoretical basis for developing more effective osteoporosis treatment strategies.

Acknowledgements

Not applicable.

Funding

The present study was supported by the Central Government-Guided Local Science and Technology Development Foundation of Hebei Province (grant nos. 226Z7709G and 246Z7744G), the Natural Science Foundation of Hebei Province (grant no. H2022209054) and the Basic Scientific

Research Foundation of Universities in Hebei Province (grant no. JYG2021005).

Availability of data and materials

The data generated in the present study may be requested from the corresponding author.

Authors' contributions

FT and JG conceived and designed the study, supervised the project, interpreted the data, critically revised the manuscript for important intellectual content and approved the final manuscript. FT and JG are responsible for the overall integrity of the work. HY made substantial contributions to the conception of the work, performed all experiments, analyzed and interpreted the data, drafted the manuscript and approved the final version. JG and HY confirm the authenticity of all raw data. QL and YH made substantial contributions to data acquisition, performed the statistical analysis, interpreted the results and approved the final manuscript. ZY contributed to data collection, validation of the experimental results and approval of the final manuscript. LX, YX and XH performed the H&E and TRAP staining experiments, contributed to the analysis and interpretation of the histological data, and approved the final manuscript. DH secured funding for the study, provided methodological guidance, contributed to the critical review of the manuscript and approved the final version. All authors have read and approved the final manuscript, and agree to be accountable for all aspects of the work.

Ethics approval and consent to participate

All experiments were approved by the Institutional Animal Care and Use Committee of North China University of Science and Technology (Tangshan, China; approval no. 2023-SY-230).

Patient consent for publication

Not applicable.

Competing interests

The authors declare that they have no competing interests.

References

1. Gao HX, Regier EE and Close KL: International diabetes federation world diabetes Congress 2015. J Diabetes 8: 300-302, 2016.
2. Carballido-Gamio J: Imaging techniques to study diabetic bone disease. Curr Opin Endocrinol Diabetes Obes 29: 350-360, 2022.
3. Liu X, Chen F, Liu L and Zhang Q: Prevalence of osteoporosis in patients with diabetes mellitus: A systematic review and meta-analysis of observational studies. BMC Endocr Disord 23: 1, 2023.
4. Schacter GI and Leslie WD: Diabetes and osteoporosis: Part I, epidemiology and pathophysiology. Endocrinol Metab Clin North Am 50: 275-228, 20215.
5. Vilaca T, Schini M, Harnan S, Sutton A, Poku E, Allen IE, Cummings SR and Eastell R: The risk of hip and non-vertebral fractures in type 1 and type 2 diabetes: A systematic review and meta-analysis update. Bone 137: 115457, 2020.
6. Asadipooya K and UY EM: Advanced glycation end products (AGEs), receptor for AGEs, diabetes, and bone: Review of the literature. J Endocr Soc 3: 1799-1818, 2019.
7. Yamagishi S: Role of advanced glycation end products (AGEs) in osteoporosis in diabetes. Curr Drug Targets 12: 2096-2102, 2011.
8. Lee HS and Hwang JS: Impact of type 2 diabetes mellitus and antidiabetic medications on bone metabolism. Curr Diab Rep 20: 78, 2020.
9. Napoli N, Chandran M, Pierroz DD, Abrahamsen B, Schwartz AV and Ferrari SL; IOF Bone and Diabetes Working Group: Mechanisms of diabetes mellitus-induced bone fragility. Nat Rev Endocrinol 13: 208-219, 2017.
10. Jankovic J: Complications and limitations of drug therapy for Parkinson's disease. Neurology 55 (12 Suppl 6): S2-S6, 2000.
11. Pietschmann P, Patsch JM and Schernthaner G: Diabetes and bone. Horm Metab Res 42: 763-768, 2010.
12. Holstege A: Long-term drug treatments to improve prognosis of patients with liver cirrhosis and to prevent complications due to portal hypertension. Z Gastroenterol 57: 983-996, 2019 (In German).
13. Huang KC, Chuang PY, Yang TY, Tsai YH, Li YY and Chang SF: Diabetic rats induced using a high-fat diet and low-dose streptozotocin treatment exhibit gut microbiota dysbiosis and osteoporotic bone pathologies. Nutrients 16: 1220, 2024.
14. Boyar H, Turan B and Severcan F: FTIR spectroscopic investigation of mineral structure of streptozotocin induced diabetic rat femur and tibia, Spectroscopy 17: 627–633, 2003.
15. Lu R, Zheng Z, Yin Y and Jiang Z: Genistein prevents bone loss in type 2 diabetic rats induced by streptozotocin. Food Nutr Res 64: 10.29219/fnr.v64.3666, 2020.
16. Wu X, Gong H, Hu X, Shi P, Cen H and Li C: Effect of verapamil on bone mass, microstructure and mechanical properties in type 2 diabetes mellitus rats. BMC Musculoskelet Disord 23: 363, 2022.
17. Ghodsi R and Kheirouri S: Carnosine and advanced glycation end products: A systematic review. Amino Acids 50: 1177-1186, 2018.
18. Corona C, Frazzini V, Silvestri E, Lattanzio R, La Sorda R, Piantelli M, Canzoniero LM, Ciavardelli D, Rizzarelli E and Sensi SL: Effects of dietary supplementation of carnosine on mitochondrial dysfunction, amyloid pathology, and cognitive deficits in 3xTg-AD mice. PLoS One 6: e17971, 2011.
19. Jukić I, Kolobarić N, Stupin A, Matić A, Kozina N, Mihaljević Z, Mihalj M, Šušnjara P, Stupin M, Ćurić ŽB, *et al*: Carnosine, small but mighty-prospect of use as functional ingredient for functional food formulation. Antioxidants (Basel) 10: 1037, 2021.
20. Ko EA, Park YJ, Yoon DS, Lee KM, Kim J, Jung S, Lee JW and Park KH: Drug repositioning of polaprezinc for bone fracture healing. Commun Biol 5: 462, 2022.
21. Busa P, Lee SO, Huang N, Kuthati Y and Wong CS: Carnosine alleviates knee osteoarthritis and promotes synoviocyte protection via activating the Nrf2/HO-1 signaling pathway: An in-vivo and in-vitro study. Antioxidants (Basel) 11: 1209, 2022.
22. Huang T, Yan G and Guan M: Zinc homeostasis in bone: Zinc transporters and bone diseases. Int J Mol Sci 21: 1236, 2020.
23. Kheirouri S, Alizadeh M and Maleki V: Zinc against advanced glycation end products. Clin Exp Pharmacol Physiol 45: 491-498, 2018.
24. Marreiro DD, Cruz KJ, Morais JB, Beserra JB, Severo JS and de Oliveira AR: Zinc and oxidative stress: Current mechanisms. Antioxidants (Basel) 6: 24, 2017.
25. Brzóska MM and Rogalska J: Protective effect of zinc supplementation against cadmium-induced oxidative stress and the RANK/RANKL/OPG system imbalance in the bone tissue of rats. Toxicol Appl Pharmacol 272: 208-220, 2013.
26. Bartmański M, Pawłowski Ł, Knabe A, Mania S, Banach-Kopeć A, Sakowicz-Burkiewicz M and Ronowska A: The effect of marginal Zn(2+) excess released from titanium coating on differentiation of human osteoblastic cells. ACS Appl Mater Interfaces 16: 48412-48427, 2024.
27. Shiota J, Tagawa H, Izumi N, Higashikawa S and Kasahara H: Effect of zinc supplementation on bone formation in hemodialysis patients with normal or low turnover bone. Ren Fail 37: 57-60, 2015.
28. Saito M and Marumo K: Collagen cross-links as a determinant of bone quality: A possible explanation for bone fragility in aging, osteoporosis, and diabetes mellitus. Osteoporos Int 21: 195-214, 2010.
29. Yudhani RD, Pakha DN, Wiyono N and Wasita B: Molecular mechanisms of zinc in alleviating obesity: Recent updates (Review). World Acad Sci J 6: 70, 20242024.

30. Gao X, Al-Baadani MA, Wu M, Tong N, Shen X, Ding X and Liu J: Study on the local anti-osteoporosis effect of polaprezinc-loaded antioxidant electrospun membrane. Int J Nanomedicine 17: 17-29, 2022.
31. An Y, Zhang H, Wang C, Jiao F, Xu H, Wang X, Luan W, Ma F, Ni L, Tang X, *et al*: Activation of ROS/MAPKs/NF-κB/NLRP3 and inhibition of efferocytosis in osteoclast-mediated diabetic osteoporosis. FASEB J 33: 12515-201927, 2019.
32. Li M, Sun Z, Zhang H and Liu Z: Recent advances on polaprezinc for medical use (Review). Exp Ther Med 22: 1445, 2021.
33. Furman BL: Streptozotocin-induced diabetic models in mice and rats. Curr Protoc Pharmacol 70: 5.47.1-5.20, 2015.
34. Furman BL: Streptozotocin-induced diabetic models in mice and rats. Curr Protoc 1: e78, 2021.
35. Islam MS and Loots DT: Experimental rodent models of type 2 diabetes: A review. Methods Find Exp Clin Pharmacol 31: 249-261, 2009.
36. Amri J, Alaee M, Babaei R, Salemi Z, Meshkani R, Ghazavi A, Akbari A and Salehi M: Biochanin-A has antidiabetic, antihyperlipidemic, antioxidant, and protective effects on diabetic nephropathy via suppression of TGF-β1 and PAR-2 genes expression in kidney tissues of STZ-induced diabetic rats. Biotechnol Appl Biochem 69: 2112-2121, 2022.
37. Muhammad HJ, Shimada T, Fujita A and Sai Y: Sodium citrate buffer improves pazopanib solubility and absorption in gastric acid-suppressed rat model. Drug Metab Pharmacokinet 55: 100995, 2024.
38. Krebs H: Citric acid cycle: A chemical reaction for life. Nurs Mirror 149: 30-32, 1979.
39. Sun Q, Tian FM, Liu F, Fang JK, Hu YP, Lian QQ, Zhou Z and Zhang L: Denosumab alleviates intervertebral disc degeneration adjacent to lumbar fusion by inhibiting endplate osteochondral remodeling and vertebral osteoporosis in ovariectomized rats. Arthritis Res Ther 23: 152, 2021.
40. Livák F and Petrie HT: Somatic generation of antigen-receptor diversity: A reprise. Trends Immunol 22: 608-612, 2001.
41. Tsuji-Naito K: Aldehydic components of cinnamon bark extract suppresses RANKL-induced osteoclastogenesis through NFATc1 downregulation. Bioorg Med Chem 16: 9176-9183, 2008.
42. Matsui S, Hiraishi C, Sato R, Kojima T, Matoba K, Fujimoto K and Yoshida H: Association of metformin administration with the serum levels of zinc and homocysteine in patients with type 2 diabetes: A cross-sectional study. Diabetol Int 16: 394-402, 2025.
43. Goyal SN, Reddy NM, Patil KR, Nakhate KT, Ojha S, Patil CR and Agrawal YO: Challenges and issues with streptozotocin-induced diabetes-A clinically relevant animal model to understand the diabetes pathogenesis and evaluate therapeutics. Chem Biol Interact 244: 49-63, 2016.
44. El Dib R, Gameiro OL, Ogata MS, Módolo NS, Braz LG, Jorge EC, do Nascimento P Jr and Beletate V: Zinc supplementation for the prevention of type 2 diabetes mellitus in adults with insulin resistance. Cochrane Database Syst Rev 2015: CD005525, 2015.
45. Sureshkumar K, Durairaj M, Srinivasan K, Goh2 KW, Undela K, Mahalingam VT, Ardianto C, Ming LC and Ganesan RM: Effect of L-carnosine in patients with age-related diseases: A systematic review and meta-analysis. Front Biosci (Landmark Ed) 28: 18, 2023.
46. Cararo JH, Streck EL, Schuck PF and Ferreira Gda C: Carnosine and related peptides: Therapeutic potential in age-related disorders. Aging Dis 6: 369-379, 2015.
47. Yamaguchi M and Ehara Y: Zinc decrease and bone metabolism in the femoral-metaphyseal tissues of rats with skeletal unloading. Calcif Tissue Int 57: 218-223, 1995.
48. Sugiyama T, Tanaka H and Kawai S: Improvement of periarticular osteoporosis in postmenopausal women with rheumatoid arthritis by beta-alanyl-L-histidinato zinc: A pilot study. J Bone Miner Metab 18: 335-338, 2000.
49. Kato H, Ochiai-Shino H, Onoder S, Saito A, Shibahara T and Azuma T: Promoting effect of 1,25(OH)2 vitamin D3 in osteogenic differentiation from induced pluripotent stem cells to osteocyte-like cells. Open Biol 5: 140201, 2015.
50. Seo HJ, Cho YE, Kim T, Shin H and Kwun IS: Zinc may increase bone formation through stimulating cell proliferation, alkaline phosphatase activity and collagen synthesis in osteoblastic MC3T3-E1 cells. Nutr Res Pract 4: 356-361, 2010.
51. Yamaguchi M, Goto M, Uchiyama S and Nakagawa T: Effect of zinc on gene expression in osteoblastic MC3T3-E1 cells: Enhancement of Runx2, OPG, and regucalcin mRNA expressions. Mol Cell Biochem 312: 157-166, 2008.
52. Yang Y, Wang Y, Kong Y, Zhang X, Zhang H, Gang Y and Bai L: Carnosine prevents type 2 diabetes-induced osteoarthritis through the ROS/NF-κB pathway. Front Pharmacol 9: 598, 2018.
53. Yamaguchi M and Uchiyama S: Receptor activator of NF-kappaB ligand-stimulated osteoclastogenesis in mouse marrow culture is suppressed by zinc in vitro. Int J Mol Med 14: 81-85, 2004.
54. Thomas S and Jaganathan BG: Signaling network regulating osteogenesis in mesenchymal stem cells. J Cell Commun Signal 16: 47-61, 2022.
55. Amarasekara DS, Kim S and Rho J: Regulation of osteoblast differentiation by cytokine networks. Int J Mol Sci 22: 2851, 2021.
56. Lin W, Hu S, Li K, Shi Y, Pan C, Xu Z, Li D, Wang H, Li B and Chen H: Breaking osteoclast-acid vicious cycle to rescue osteoporosis via an acid responsive organic framework-based neutralizing and gene editing platform. Small 20: e2307595, 2024.
57. Amin N, Clark CCT, Taghizadeh M and Djafarnejad S: Zinc supplements and bone health: The role of the RANKL-RANK axis as a therapeutic target. J Trace Elem Med Biol 57: 126417, 2020.
58. Molenda M and Kolmas J: The role of zinc in bone tissue health and regeneration-a review. Biol Trace Elem Res 201: 5640-5651, 2023.
59. Ono T, Hayashi M, Sasaki F and Nakashima T: RANKL biology: Bone metabolism, the immune system, and beyond. Inflamm Regen 40: 2, 2020.
60. Boyce BF and Xing L: Functions of RANKL/RANK/OPG in bone modeling and remodeling. Arch Biochem Biophys 473: 139-146, 2008.